Numerical simulation of liquid composite molding processes

Joël Bréard — **Abdelghani Saouab**

Laboratoire de Mécanique, Physique et Géosciences, Université du Havre
Quai Frissard, BP 540, F-76058 Le Havre cedex

{joel.breard, abdelghani.saouab}@univ-lehavre.fr

ABSTRACT. *This work proposes to perform an analysis about the numerical simulation of LCM processes. After a description of the modelling context of these processes, our first part will describe the formulation of the laws, and a second step the application with the Thermo-Hydro-Mechanical coupling. We present a finite element procedure to simulate mold filling in the three dimensional case. The method presented in the paper is div-conform i.e. the mass of injected fluid is proved to be perfectly conserved. Numerical results are compared with experiments. In order to take into account the micro-macro voids during the filling of the reinforcement, we introduce a phenomenon of transport in saturation corresponding to a mechanism of hydrodynamic dispersion. This study is supplemented by a study of coupling between processes and mechanical properties, insisting on the advantage of introducing the concept of saturation.*

RÉSUMÉ. *Ce travail propose de faire un état de l'art sur la simulation numérique des procédés LCM. Après avoir rappelé le contexte de la modélisation de ces procédés, nous précisons d'une part, la formulation des lois d'évolution et de comportement et, d'autre part, l'application aux couplages Thermo-Hydro-Mécanique. Nous avons présenté les éléments finis dans le cas des analyses tridimensionnelles de remplissage de cavité. Il s'avère que la méthode retenue est l'utilisation d'éléments discontinus permettant que la masse du fluide injecté soit parfaitement conservée. Ensuite des résultats numériques sont comparés aux expériences. Enfin, pour tenir compte des créations de micro-macro vides durant l'imprégnation des renforts, nous introduisons un phénomène de transport en saturation correspondant à un mécanisme de dispersion hydrodynamique. L'étude est complétée par une discussion sur le couplage entre procédés et propriétés mécaniques, en montrant l'intérêt d'y introduire la notion de saturation.*

KEYWORDS: *LCM processes, THM coupling, convection-diffusion, saturation, porous medium.*

MOTS-CLÉS : *procédés LCM, couplage THM, convection-diffusion, saturation, milieu poreux.*

Nomenclature

$\overline{\overline{C}}$, C_z	compressibility tensor, transverse compressibility
F_c , F_{clamp}	control, clamping force of the mold
F , F_{eff} , F_{geo}	intrinsic, effective, geometric constitutive law
$R_{F,S}$, F_{sat} , F_{unsat}	saturation ratio, unsaturated and saturated variable
S , f_{rel} , Q_S	variable, relative size function, sink effect of saturation
$\overline{K}$, K_{geo} , K_d	permeability tensor, geometrical and draining permeability
B , $\overline{T}$	conductance, directional conductivity of the porous channel
p , P_i , P_v	resin, injection, vent pressure
Q_i	injection flow rate
U_c	control compression rate of the mold
$\overline{D}$	hydrodynamic dispersion
V_{part} , V_{part0}	specific and initial volume of composite part
h , h_0 , Δh	thickness, thickness variation, initial thickness of the perform
$\overline{U}, \overline{V}, \overline{W}$	solid, fluid and relative of the fluid displacement
$\underline{q}$, q_r , v_n	fluid, filtration, fluid in wall velocity
$\underline{u_s}$	solid velocity
$\underline{q}''$, $\underline{j_d}$	heat, diffusive flux
c	concentration
T , T_g	resin, glass transition temperature
c_p	specific heat of the fluid
$\dot{H}$	instantaneous heat generated by the exothermy
Pe , Ca	Peclet number, Capillary number
V_f	fiber volume content

Greek symbols

$\overline{\lambda}$	thermal conductivity tensor
λ_{chem}	total polymerization shrinkage
$\overline{\sigma}'$, σ_z	effective stress tensor, transversal total stress
$\phi, 1\phi, 2\phi$	porosity, mono and double distribution of fiber network
θ	angle orientation of fiber
α , α_{gel}	degree of curing, gelation chemical conversion
β_{gel} , β_{cured}	coefficients of thermal expansion of the gelled, fully cured resin
μ , ρ	dynamic viscosity, density of the fluid
ε_z	transverse deformation

1. Introduction

The objective of this work is to give an overall picture of the art of modelling in LCM processes. In this context, the evolution of the tools for processes simulation is an invaluable help in the decision-making when designing parts, choosing materials processes. Today some software make it possible to simulate LCM processes. This work makes it possible to formalize the problem arising from a numerical point of view and to present the various input-outputs integrated into simulations.

Traditionally, the development and the calculation of the mechanical properties of the composite structures are treated separately, for both cultural and scientific reasons. However, the development and structural properties are mutually dependant. It is important to contribute to the definition of a coupled approach, applied to LCM processes. A parameter such as the void content is common to the studies carried out on process and structure calculation, and will make it possible to define a criterion of health material. On this subject, physical mechanisms (Patel *et al.*, 1996), numerical models (Spaid *et al.*, 1998), (Bréard *et al.*, 2003b) and experimental measurements (Labat *et al.*, 2001) were studied.

In this work, we present the results based on the analysis of unsaturated/saturated flows through a porous media with double porosity (Bréard *et al.*, 2003a), while completing with the couplings Thermo-Hydro-Mechanics (THM) implied in LCM processes (Bréard, 2004). In what follows, our work is divided into five great parts: presentation of the various families of processes; the modelling of THM couplings; numerical method employed; some simulations and a presentation of the criteria within the framework of the process – structure couplings.

2. Presentation of the family of LCM processes

2.1. *The various initials*

Within the framework of processes LCM (Composite Liquid Molding), we made the choice present the following techniques. This list is not exhaustive:

RTM	(Resin Transfer Molding)
VARTM	(Vacuum Assisted Resin Transfer Molding)
CRTM	(Compression Resin Transfer Molding)
RTM Light	(Resin Transfer Molding Light)
FASTRAC	(FAST Remotely Actuated Channeling)
LRI	(Liquid Resin Infusion)
SCRIMP	(Seemann Composites Resin Infusion Molding Process)
VARI/VARIM	(Vacuum Assisted Resin Infusion Molding)
RFI	(Resin Film Infusion)

We can thus distinguish two great families: injection by transfer of resin (RTM and variants of the process) and infusion by resin infiltration (Infusion and variants), as presented on Figure 1, with boundary conditions.
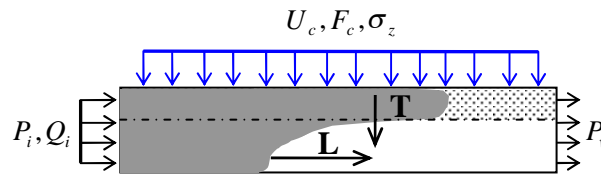

Figure 1. *Representative diagram of the LCM processes families L: Longitudinal flow, T: Transversal flow*

2.2. *Description of the processes*

The various conditions can be summarized in Table 1. The mold is defined according to three categories: rigid, semi-rigid and flexible. These walls can be controlled while under stress, or in displacement. During injection, the filling develops according to three mechanisms: Longitudinal (L), Longitudinal-Transversal (L+T), Transversal (T). Lastly, injection or infusion is controlled by the boundary conditions with injection and vent sealed with the atmospheric pressure: < 1 (vacuum), 1 (atmospheric pressure), > 1 (injection pressure).
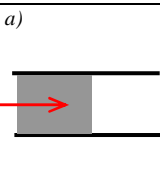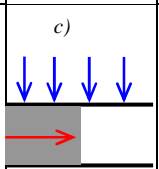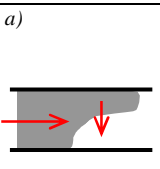
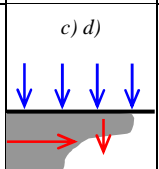**Table 1.** *Processes parameters*
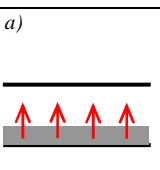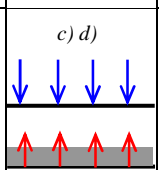
Process	Mold Control	Mold	Vent pressure	Injection pressure	Front	Draining
RFI	Stress	Flexible	1	1	T	No
LRI	Stress	Flexible	<1	1	L+T	Preform (1) (2)
SCRIMP	Stress	Flexible	<1	1	L+T	Net bleeder (1)
VARI/VARIM	Stress	Flexible	<1	1	L	No
FASTRAC	Stress	2 bags	<1	>1	L+T	Channel
RTM Light	Stress	Semi-rigid	1	>1	L	Preform (2)
VARTM	Fixed gap	Rigid	<1	>1	L	No
RTM	Fixed gap	Rigid	1	>1	L	No
CRTM	Displacement	Rigid	<1	>1	L + T	Channel

(1) External : consumable, (2) Internal : integrated into the finished structure

2.3. *Classification of the processes*

We can then propose Table 2 of synthesis corresponding to the HydroMechanical coupling in LCM processes. We distinguish two controls: mold control (fixed gap, displacement or stress imposed) and flow control (intrinsic one: choice of the reinforcements and draining and extrinsic: condition with injection and vent). The initials [a),b),c),d)] correspond to the mass conservation equations developed with chapter 3.3.

Table 2. *Processes classification*

Mold		RTM	CRTM	RTM Light	Infusion	Process
		Rigid		semi-rigid	flexible	Infusion
Flow Control	L	a)	b) c)	c)	c)	VARI
	L + T	a)	b) c)	c) d)	c) d)	SCRIMP LRI FASTRAC
	T	a)	b) c)	c) d)	d)	RFI
Mold Control		Fixed gap	Imposed displacement or stress			

3. Modeling of THM coupling

3.1. *Process - Composite part - Structure/context*

Before developing the integration of the various laws of evolution and behavior, Figure 2 is a reminder of the framework of the Process – Composite part – Structure coupling.
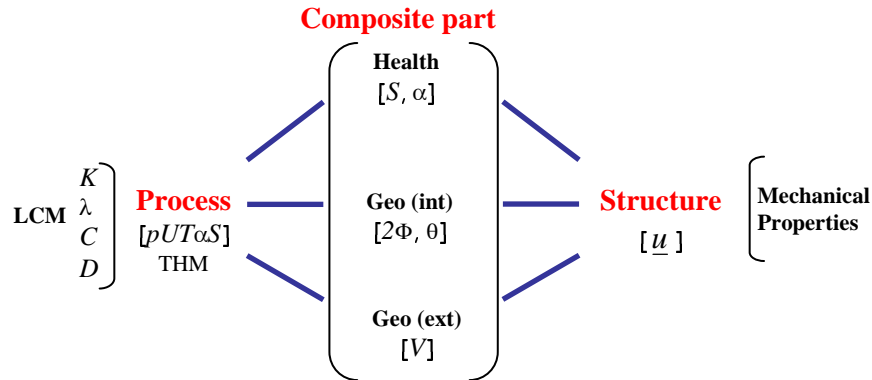
Composite part

Health
[*S*, α]

Geo (int)
[*2Φ*, θ]

Geo (ext)
[*V*]

$\left.\begin{matrix} K \\ \lambda \\ C \\ D \end{matrix}\right\}$ **LCM**

Process
[*pUT*αS]
THM

Structure
[*u*]

Mechanical
Properties

Figure 2. *« Process – Composite part – Structure » context*

The process modeling will be summarized in an [*pUT*α*S*] approach and will be a particular analysis of THM couplings. We define three variables "Composite part" represented respectively by health material [α,*S*], internal geometry [*2Φ*,θ] and external geometry [*V*]. 2Φ describe the distribution of fiber network. For the structural approach, we use the traditional elements of the structural analysis. For the process approach, the various variables associated with the coupling THM, are defined in the system of equations [1].

$$\begin{Bmatrix} \underline{\underline{q}} \\ \underline{\sigma}' \\ \underline{q}'' \\ \underline{j_d} \end{Bmatrix} = \begin{bmatrix} \overline{K} & & & \\ & \overline{\overline{C}} & & \\ & & \overline{\lambda} & \\ & & & \overline{D} \end{bmatrix} \begin{Bmatrix} \underline{\nabla}p \\ \underline{\nabla}U \\ \underline{\nabla}T \\ \underline{\nabla}c \end{Bmatrix} \qquad [1]$$

3.2. *THM context*

As had specified we previously, the processes are the subject of a modelling based on THM couplings in porous media. The formulation is defined *via* an approach the [*pUT*α*S*] type (Figure 3).

To give an overall view of the formula, let us note the field *e* and *d* its associated dual field. The whole of the physical problems linked to the process can thus be summarized by the problem to solve according to:

$$\begin{cases} \underline{\nabla} \cdot \underline{d} = \psi \\ \underline{d} = \overline{F_{eff}} \, \underline{\nabla}e \end{cases} \qquad [2]$$

With the volumic source term

$$\psi = \delta_0 + \alpha_0 \frac{\partial e}{\partial t} + \beta_0 \underline{q} \cdot \underline{\nabla} e \qquad [3]$$

where $\alpha_0, \beta_0, \delta_0$ will be defined according to the model. In [2], we define the effective constitutive law $\overline{F_{eff}}$ like a function dependent on three components, respectively on the convective effect, health material and intrinsic component.

$$\overline{F_{eff}} = f(Pe, \alpha, S, B, \overline{T}) \qquad [4]$$

Then, it is possible to define the relations representing the physics of LCM processes, while being based on a description with the concept of continuous mediums (Bear, 1990; Coussy, 1991).
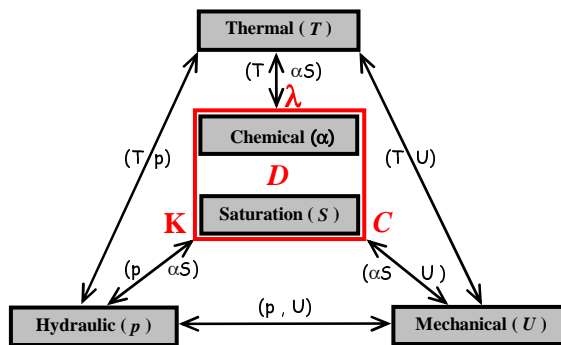

Figure 3. *THM coupling of the processes*

3.2.1. *Mass conservation*

Since both the liquid and solid phases are incompressible, the corresponding mass conservation equations (Tucker *et al.*, 1996; Bréard *et al.*, 2003a) can be written as:

$$\begin{cases} fluid : & \dfrac{\partial \phi S}{\partial t} + \nabla \cdot (\phi S \dfrac{\partial \underline{V}}{\partial t}) = 0 & (a) \\ solid : & \dfrac{\partial (1 - \phi S)}{\partial t} + \nabla \cdot ((1 - \phi S) \dfrac{\partial \underline{U}}{\partial t}) = 0 & (b) \end{cases} \qquad [5]$$

The continuity equation for the whole domain is obtained by summing the two members of the above equations. By using [5], with $\underline{V} = \underline{W} + \underline{U}$, we obtain:

$$\frac{\partial \phi S}{\partial t} + \nabla \cdot (\phi S \frac{\partial \underline{W}}{\partial t} + \phi S \frac{\partial \underline{U}}{\partial t}) = 0 \qquad [6]$$

With the velocities expression, we deduce the following:

$$\frac{\partial \phi S}{\partial t} + \nabla \cdot \underline{q} + \phi S \nabla \cdot \underline{u}_s + \underline{u}_s \cdot \nabla \phi S = 0 \qquad [7]$$

If we introduce the material derivative with

$$\frac{D_s(..)}{Dt} = \frac{\partial(..)}{\partial t} + \underline{u}_s \cdot \nabla(..) \qquad [8]$$

The equation [7] for the liquid phase becomes

$$\frac{D_s(\phi S)}{Dt} + \nabla \cdot \underline{q} + (\phi S)\nabla \cdot \underline{u}_s = 0 \qquad [9]$$

And from [8] for the solid phase, we obtain

$$\frac{D_s(1-\phi S)}{Dt} + (1-\phi S)\nabla \cdot \underline{u}_s = 0 \qquad [10]$$

By subtracting [10] with [9], we obtain finally the equation of following continuity:

$$\nabla \cdot \underline{q} = -\frac{1}{1-\phi S} \frac{D_s(\phi S)}{Dt} \qquad [11]$$

3.2.2. *Balance of momentum*

The fluid flows towards the exterior through the surface Γ of a porous medium containing a fluid phase $\phi \Gamma$ and a solid phase $(1-\phi)\Gamma$. The filtration velocity $q_r = \frac{\partial W}{\partial t}$ is defined from the filtration vector. The flow q per unit surface (Darcy velocity) can be expressed from the filtration velocity q_r by the relation

$$\underline{q} = \phi \frac{\partial \underline{W}}{\partial t} = -\frac{\overline{K}}{\mu} \nabla p \qquad [12]$$

Darcy's law, both from the experimental and theoretical points of view, is valid in permanent regime and saturated flow. It is very often applied also to unsaturated

flows. This means that these flows are considered as quasi-stationary, *i.e.*, as a succession of flows in permanent regime. In other cases of regime, some conditions may also be taken into account: non-newtonian behavior, transient term.

3.2.3. *Equation of energy and chemical kinetics*

Because of resin exothermy, energy transferred by conduction from the walls from the mould and the convective energy by the resin flow, the phenomena of heat transfer cannot be neglected during the filling of the processes (Ngo *et al.*, 2001), (Ruiz, 2004). In addition, the viscosity of the thermoset resin systems changes according to the temperature and the degree of polymerization (Ryan. *et al.*, 1979), (Blest *et al.*, 1999). From the assumption of a model of local balance in temperature, we obtain the equation of following energy:

$$\rho c_p \frac{\partial T}{\partial t} + \rho_r c_{p_r} \frac{q}{\phi} \nabla T = \nabla \cdot \bar{\lambda} \nabla T + \frac{Dp}{dt} + \phi \rho_r \dot{H} \qquad [13]$$

The term of exothermy is defined by the reaction rate (Bailleul *et al.*, 2003).

$$\frac{\partial \alpha}{\partial t} + \frac{q}{\phi} \nabla \alpha = \dot{H} \qquad [14]$$

These modifications of temperature and degree of polymerization will involve a modification of viscosity (Ruiz, 2004) according to the following relation

$$\mu(T,\alpha) = C_T \exp\left(\frac{T_g}{T}\right) \left(\frac{\alpha_{gel}}{\alpha_{gel} - \alpha}\right)^{C_1 + C_2 \alpha} \qquad [15]$$

3.2.4. *Volume changes*

During curing, a variation of the part volume could be due to the changes of temperature and degree of polymerization (Hill *et al.,* 1995; Ruiz, 2004). This change can be represented by the following relation

$$\left(\frac{1}{V_0}\frac{dV}{dt}\right)_{overall} = \left(\frac{1}{V_0}\frac{dV}{dt}\right)_{\substack{thermal \\ contribution}} - \left(\frac{1}{V_0}\frac{dV}{dt}\right)_{\substack{polymerization \\ shinkage}} \qquad [16]$$

with

$$\left(\frac{1}{V_0}\frac{dV}{dt}\right)_{\substack{thermal \\ contribution}} = \beta_{gel}\frac{dT}{dt} + (\beta_{cured} - \beta_{gel})\alpha\frac{dT}{dt} \text{ and } \left(\frac{1}{V_0}\frac{dV}{dt}\right)_{\substack{polymerization \\ shinkage}} = \lambda_{chem}\frac{dT}{dt}$$

3.2.5. *Equilibrium relationships*

The Terzaghi's law assumes that the fluid action can be modeled like an external force acting on the solid skeleton. This law leads to the following equilibrium relation:

$$\nabla \cdot \overline{\sigma}' - \nabla p = \underline{\varphi}(S) \qquad [17]$$

In which the action of the fluid on the solid part is transmitted by volume forces of intensity $-\nabla p$, $\overline{\sigma}'$ being the effective stress acting on the skeleton. This decoupling hypothesis enables us to study large fluid motions independently of the small strains that occur in the skeleton. This effective stress is in direct relationship to the characteristics of compressibility of the medium

$$\overline{\sigma}' = \overline{\overline{C}}\,\overline{\varepsilon} \qquad [18]$$

Other behavior laws can be introduced: viscoelasticity and the taking into account of saturation and thermal effects.

3.2.6. *Behavior laws : permeability, thermal conductivity and compressibility*

The permeability, thermal conductivity and compressibility are defined like functions of saturation and intrinsic characteristic of the medium, such as:

$$F(S) = f_{rel}(S)F_{geo} \qquad [19]$$

where F is a variable corresponding to $\overline{K}, \overline{\lambda}, \overline{\overline{C}}$. The term $f_{rel}(S)$ is a relative size function of saturation, where $R_{F,S} \leq f_{rel}(S) \leq 1$, with F_S the ratio between the unsaturated and saturated variable, such as $R_{F,S} = \dfrac{F_{unsat}}{F_{sat}}$. We define for the relative function a power law by the relation $f_{rel}(S) = [(1 - R_{F,S}^{*})S + R_{F,S}^{*}]^{\beta_F}$ where β_F is a constant and $R_{F,S}^{*} = R_{F,S}^{\frac{1}{\beta_F}}$.

Simulation requires that we should specify the behaviour laws. Many works on this subject can be classified in three great families: i) empirical measurement (macroscopic/phenomenological), ii) analytical and semi-analytical modelisation (micro-mesoscopic) and iii) numerical simulation (FE and LBE methods). We can quote the work of (Binétruy, 1996; Bréard, 2004; Pitchumani *et al.*, 1999; Cadinot, 2002; Chen *et al.*, 2001) for the analytical one, (Fournier, 2003), (Torres *et al.*, 2001) for FEM and (Spaid *et al.*, 1998), (Lomov *et al.*, 2001) for LBE.

3.2.7. *Boundary conditions of HM coupling problem*

We now state the boundary conditions that govern a permanent flow through a deformable porous medium. Combining [11] and [12] together with [17] gives the three equations that express the coupling between the flow, the deformation in a porous medium and the saturation.

$$
\begin{cases}
\nabla \cdot \overline{\sigma}'(U_i) = \nabla p + \underline{\varphi}(S) \\
\nabla \cdot \left(\dfrac{\overline{K}(S)}{\mu} \nabla p \right) = \dfrac{1}{1 - S\phi} \dfrac{D_s}{Dt} S\phi(\underline{U}) \\
\dfrac{\partial S}{\partial t} + \dfrac{q}{\phi} \nabla S = g(S)
\end{cases}
\tag{20}
$$

The unknowns in this system are the pore pressure p, the displacement of the solid phase $\underline{U}$ and the saturation S, and are related to M and T. The boundary conditions depend on each particular problem which we develop in chapter 4.

3.3. *Analyzed case: HM coupling*

To finish this presentation about the processes modelling, we will continue on HM couplings. This study implies the analysis of two cases of boundary conditions, applied to the transversal study of compressibility:

– imposed displacement (U_c): CRTM application (with rigid mould),

– imposed stress (σ): in the case of the clamping forces, CRTM application (with rigid mould) or in the case of vacuum stress, VARI, LRI or RFI applications (with flexible mould). We will be able to analyze the numerical tools on the basis of following main equation:

$$
\nabla \cdot \underline{q} = -\frac{1}{1 - \phi S} \frac{D_s(\phi S)}{Dt}
\tag{21}
$$

The following equations present the general framework of modelling defined in Table 2. The results which we present in this work result from various numerical work of which a part obtained with software PAMRTM™, in which we have to take part to develop and to validate the RTM (*a*) and the VARI (*c*).

$$
a) \qquad \nabla \cdot \underline{q} = -\phi \frac{\partial S}{\partial t}
$$

$$b) \quad \nabla \cdot \underline{q} = -\frac{U_c}{h(t)} \tag{22}$$

$$c) \quad \nabla \cdot \underline{q} = \frac{1}{1-\phi S}\frac{\partial(\phi S)}{\partial t} = -\frac{\partial}{\partial t}\varepsilon_z$$

$$d) \quad \nabla \cdot \underline{q} = \frac{1}{1-\phi S}\left[\frac{\partial(\phi S)}{\partial t} + \underline{u}_S \cdot \nabla(\phi S)\right]$$

with $\Delta h = h - h_0$ and $\varepsilon_z = \dfrac{\Delta h}{h_0}$ ($\Delta h = U_c t$ for an imposed displacement). The implementation of the various techniques and variables can be gathered in a parameter of following control:

$$x = \left(K_d, \begin{bmatrix} \overline{K} \\ C_z \end{bmatrix}, \begin{bmatrix} U_c \\ \sigma_z, P_v \end{bmatrix}, \begin{bmatrix} P_i, Q_i \\ P_v \end{bmatrix} \right) \tag{23}$$

This one is represented in Table 3, by taking again four characteristics of control.

Table 3. *Boundary and initials conditions of the various processes*

Process	RTM	VARTM	CRTM	RTMlight	FASTRAC	LRI SCRIMP	VARI VARIM	RFI
Draining K_d	0	0	Channel	0	Channel	Net bleeder Preform	0	0
P_i	P_i	P_i	P_i	P_i	P_i	0	0	0
P_v	0	P_v	0	0	P_v	P_v	P_v	0
U_c	0	0	U_c	0	0	0	0	0
σ_z / P_v				P_v	P_v	P_v	P_v	F_{clamp}

4. Numerical method

There are various methods to describe the dynamics of front advancement: Lagrangian, Arbitrary Lagrangian-Eulerian (ALE), Marker-And-Cell (MAC), Volume of Fluid (VOF), … . Classically, the modelling of the cavity filling Ω with a fluid is divided into two areas, Ω_1 for the flow area and Ω_2 the area corresponding to the dry reinforcement (Figure 4). The problem of Darcy - Terzaghi - Saturation coupling is connected with the problem of the consolidation (Coussy, 1991). On the boundaries, three sets of conditions are considered as illustrated on Figure 4.

The first two sets are composed by three complementary parts:

For balance relation :

Γ_u : reinforcement displacement $\underline{u} = \langle \overline{u} \rangle$, Γ_T : surfacic force $\underline{T} = \langle \overline{T} \rangle = \overline{\sigma}\underline{n}$ and Γ_g : global force $\underline{F} = \int\limits_{\Gamma_g} \underline{T} d\Gamma$

For mass conservation:

Γ_p : pressure $P_i = \langle p \rangle$, Γ_v : velocity in wall $v_n = \underline{v}\underline{n}$ and Γ_q : flow rate $Q_i = \int\limits_{\Gamma_q} \underline{v}\underline{n} d\Gamma$

Finally for the saturation transport equation, we consider the boundary conditions with the injection $S = 1$ and the vent $\dfrac{\partial S}{\partial n} = 0$ and initial to Ω : $S = 0$.

4.1. *Flow model*

Initially, we must know the distribution of the fluid velocity in the cavity: it constitutes the filling model (Gao *et al*., 1993; Bruschke *et al*., 1994; Maier *et al*., 1996). Within this framework, we make the assumption of a model without saturation, the fluid is present only in the area Ω_1 of the cavity delimited by the walls, the injection gate and the flow front.
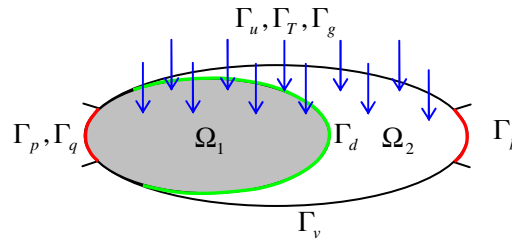

Figure 4. *Boundary conditions for processes modelling*

Then the model to be solved is a traditional problem in pressure

$$\nabla \cdot \overline{K} \nabla p = 0 \qquad\qquad [24]$$

As the fluid velocity is known, we must estimate the evolution of the resin front.

4.2. *Front advancement model*

We define in Ω a scalar field f which value is equal to one when the resin is present (saturated medium) and equal to zero when it is not (dry medium). This scalar represents the resin concentration in the porous medium. The concentration is transported in the flow and is solved by a transport equation:

$$\frac{\partial f}{\partial t} + v\nabla f = 0 \qquad [25]$$

If the fluid is reactive, its chemical properties will be also transported. Finally, if the problem is not isothermal, we must also transport the temperature of particles.

4.3. *Numerical techniques*

To solve our various physical problems, the transport formulations can be written (Bruschke *et al.,* 1994), (Kang *et al.,* 1999), (Ruiz, 2004). By defining a function test equal to the scalar potential G to be determined and while introducing a space of functions of form w the preceding equations can be summed up by the following weak formulations, summarized in two great families with F the constitutive law, f the source term and, G^+, G^- the two values of the scalar on the two sides of the boundary Γ_d :

– The diffusive equation:

$$\int_\Omega \nabla w \cdot F\nabla G d\Omega + \int_{\Gamma_d} wn \cdot q d\Gamma_d = \int_\Omega wf d\Omega \qquad [26]$$

– The transport equation:

$$\int_\Omega w\left(\frac{\partial G}{\partial t} + q\nabla G\right)d\Omega = \int_\Omega wf d\Omega + \int_{\Gamma_d} \left|G^+ - G^-\right|(n \cdot q)d\Gamma_d \qquad [27]$$

The problem [26] is traditional and corresponds to the resolution of a linear problem. It is solved by a standard Galerkin formulation. For the method [27], a Lesaint-Raviart formulation is employed (Ruiz, 2004).

4.4. *Mass conservation*

Classically, the finite element methods do not make it possible to satisfy the mass conservation when the formulation of the continuous functions on the pressure is

used to solve the problem. Indeed, the conservation equation is solved weakly, *i.e.* that the field velocity is not in its natural function space where the normal component of velocity is continuous. To take this into account, we will quantify the resin flow lost between 2-D and 3-D calculus.

A sufficient condition for div-conform approximation is that the normal component velocity is continuous on the whole of the field. We will consider a mesh M of # E elements, # F faces and # N nodes. By using this mesh, we consider the set $S^0(M)$ of all the approximations space where q is constant in each element. With this assumption, the normal component velocity is continuous everywhere except on the faces between the elements. So that an approximation is div-conform, of the constraints on # F were forced to ensure div-conformity (Remacle *et al.*, 1998).

The natural choice for div-conform element is a space N_f of dimension dim $N_f = \#F$. In this case, we have exactly the good number of degrees of freedom in the interpolation to ensure the div-conformity. From now on, the resolution of the equation [26] is equivalent to a strong continuity of the normal component velocity. Other elements of analyses are described in (Remacle *et al.*, 1999).

5. Results and discussions

We now will continue with some results of pressure validation and the problems arising within the framework of HM couplings and the modification of the transport equation for a new filling algorithm.

5.1. *Pressure validation*

We present here a comparison of calculation by using the traditional continuous elements and the discontinuous elements for 2-D and 3-D configurations. The objective is to show that the continuous 3-D solutions are not acceptable for simplified mesh. It is not the case for similar 2-D meshes. Now let us consider the problem of central injection presented on the Figure 5.
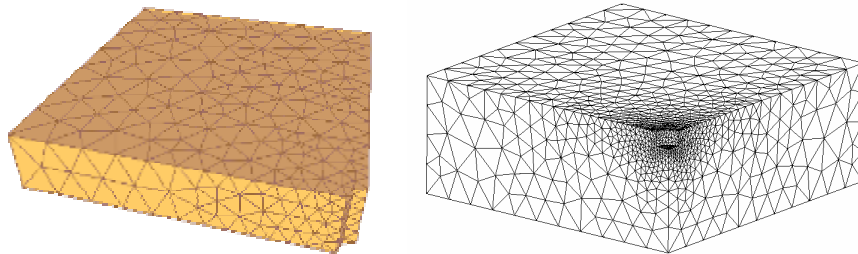

Figure 5. *Mesh for the central injection 2-D and 3-D configuration*

The mesh of Figure 5 is made of 2474 tetrahedrons (2-D) and 12490 tetrahedrons (3-D). For the 2-D injection, the problem is obviously two-dimensional and we select the upper part of the problem for a 2-D simulation. The upper mesh is made of 244 triangles. Both 2-D and 3-D configurations are calculated by using the traditional elements and the discontinuous elements. So we obtain the front flow rate and fluid losses for a 2-D calculation. We show clearly that the use of discontinuous finite element shape functions is better in term of flux conservation but the traditional continuous approximation is not to be rejected: error < 10%. In fact, it is known that the techniques of traditional finite elements are suitable for 2-D problems of mould filling (Gao *et al.*, 1993).

Now, let us consider the 3-D problem. The 2-D and 3-D meshes can be regarded as equivalent in term of density. For traditional continuous elements, we obtain the flow rate at the injection gate, at front and the loss, *i.e.* the difference between the injection and front. The solution cannot be regarded as acceptable: error < 80%. The loss is of the same order of magnitude as the injection flow rate. The difference between 2-D and 3-D computations comes down to this similar meshes, in 2-D can give acceptable results while it is not the case in 3-D. We can refine the mesh until the flow rate is sufficiently balanced but the number of time steps increases with the number of elements. The traditional continuous elements are definitively not a good solution. In the case of discontinuous elements, a perfect conservation of the flow is observed. In order to validate these results with experimental analysis, we resume the work carried out on the detection of a flow of fluid inside a opaque medium made up of glass fibers stacking. In fact, the spatial characterization of a thick reinforcement can be deduced from the determination of the front position along three principal directions.

For the front detection, we resume our work based on a radioscopy X technique (Bréard *et al.*, 1999). In this experimental device, the mould is a parallelepipedic box of dimension *30*30*2 cm³*. The injection is carried out through a cylindrical inlet (*5 mm* diameter), the fluid is a silicone oil with a viscosity of *0,1 Pa.s* in order to avoid any thermal phenomenon. The results which we present Figure 6 relate to the flow of a silicon oil injected under a pressure of *$1,89.10^5$ Pa* in a mold filled with a random mat (*porosity = 0,78*). Due to the texture of a random in-plane fibers spreading in the mat, the permeabilities are $K_X = K_Y = 3,95.10^{-10} m^2$. The permeability along the thickness direction is $K_Z = 9,3.10^{-11} m^2$ due to the anisotropy resulting from packing mats perpendicularly to the texture plane. Results present a very good agreement. The differences in the first moments are related to the fact that these transients are not taken into account by the traditional Darcy model.
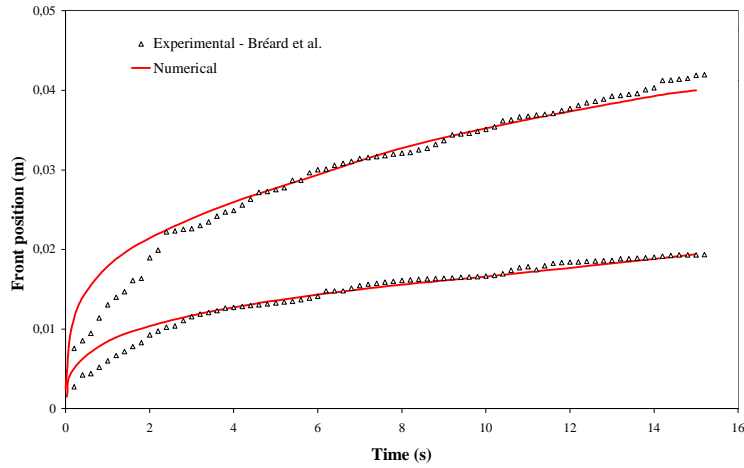
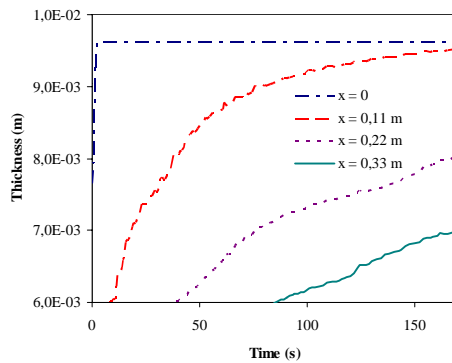**Figure 6.** *Comparison between experimental and calculation front position*

Figure 7. *Reinforcement thickness during VARI infusion*

5.2. *HydroMechanical coupling*

This part presents the first analyses carried out within the framework of HM coupling corresponding to a Darcy-Terzaghi problem without taking saturation into account. We can distinguish two configurations according to the type of wall control of the mold: rigid wall (Bickerton *et al.*, 2003) or flexible wall (Loos *et al.*, 1996), (Pham *et al.*, 1999), (Kang *et al.*, 2001). Some work considered the planar deformation of reinforcement (Farina *et al.*, 2000), (Lacoste *et al.*, 2002). In the first case, we consider the resin flow through the reinforcement with a transversal compression developed by a vacuum setting according to infusion processes VARI

or LRI. In the second case, it is a question of carrying out a flow through a reinforcement whose compression under a rigid wall is controlled either in stress, or in displacement according to CRTM processes (Saouab *et al.*, 2002a). The first problem to be solved is represented by the relation (22.c). A part of the results is presented on Figure 7 corresponding to the thickness evolution of the reinforcement, in the case of U850 reinforcement stacking of dimension *50*20 cm²*.
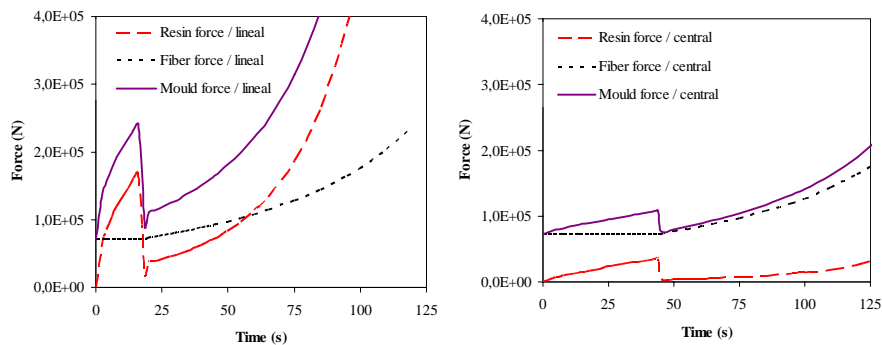

Figure 8. *Evaluation of the forces resulting on the resin, fiber and mould in a configuration CRTM with imposed displacement*

The infusion is carried out under a vacuum of *0,5.10⁵ Pa* and a fluid of viscosity $\mu = 0,92e^{0,0665t}$. The permeability and compressibility are defined by the laws $K = a(1-\phi)^b$ and $\sigma' = c(1-\phi)^d$ with $a = 9,5.10^{-12}; b = -2,64$ / $c = 1,25.10^9; d = 5,03$. The simulation configurations are defined either on the basis of elastic membrane, or of a plastic film with a coefficient of prestressed and an external pressure equivalent to P_v. It is possible to consider various scenarios, by modifying the choice of draining and the configuration on the control of compressibility in order to obtain an optimal reinforcement thickness. Experimental work made it possible to validate the first analyses (Cadinot, 2002). The following results correspond to the case of a controlled rigid wall on the one hand with displacement imposed (Figure 8) and on the other hand on imposed stress (Figure 9). The problems to be solved are represented by the relations (22.b) and (22.c) respectively with a control on displacement and stress. This analysis makes it possible to present information on the forces resulting about the resin, fibres and the mould. We more particularly present the first comparisons between a lineal injection and a central injection. Currently, this part is the subject of new developments on the infusion modelling within the framework of the RFI (Sevostianov *et al.*, 2000), (Bickerton *et al.*, 2003), (Park *et al.*, 2003) and on the problem defined by the relation (22.d).
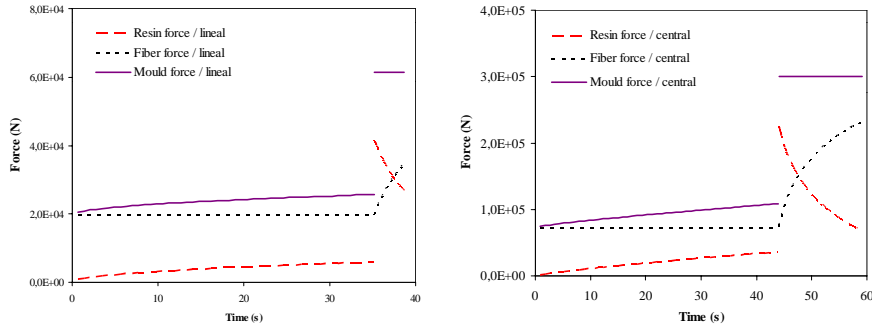
Figure 9. *Evaluation of the forces resulting on the resin, fiber and mould in a configuration CRTM with imposed stress*

5.3. *Saturation and front advancement*

The objective of this last part is the analysis of a new model for the front advancement. If we use various resins, the difference observed on the evolution of the front is mainly connected to the capillary actions which can be taken into account by the parameter of saturation (Patel *et al.*, 1996), (Acheson *et al.*, 2003). The difference between the two flow modes can be explained by the two resistance scales to the flow. The first level of resistance corresponds to the step when the fluid surrounds the tow (flow inter-tow). And, as the fluid starts to impregnate the tows (flow intra-tow), resistance to the flow decreases. A term appears in the transport equation for the saturation phase, representing the dispersion flow. The transport phenomenon corresponds to a mechanism of hydrodynamic dispersion. We can reproduce the transport of saturation (Bréard *et al.*, 2003) by the following equation:

$$\frac{\partial S}{\partial t} + \frac{q}{\phi}\nabla S = \nabla \cdot \overline{D}\nabla S - Q_S \qquad [28]$$

where, $D = f(q)$ defines the hydrodynamic effect and $Q_S = f(Ca)$ defines an air entrapment with an elliptic field (Kang *et al.*, 1999). Moreover, the velocity variations alone do not explain the evolution of the zone occupied by normal saturation with the flow direction. In this case, we must define transport by the introduction of an additional mechanism which takes seat in the tow with the form of a sink effect Q_S. It is a phenomenon of fluid accumulation in the tow with the fluid-solid interface and depends on the Capillary number. The identification of the various coefficients was carried out on the one hand with the development of saturation sensors (Labat *et al.*, 2001) and on the other hand with an analysis of the pressure behavior during the filling (Bréard *et al.*, 2003a). For example, we obtain numerical analysis of saturation as presented on Figure 10.
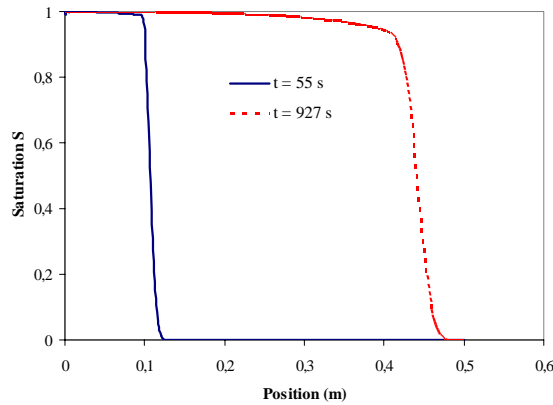
Figure 10. *Evolution of saturation transport*

This case was obtained for an injection with a pressure of 10^5 Pa, a viscosity $\mu = 0,1Pa.s$, *porosity = 0,4* and a geometrical permeability $K_{geo} = 5.10^{-11} m^2$. The mould is a parallelepipedic box of dimension *10*50*0.3 cm³* More precise details can be found in (Bréard *et al.*, 2003b). Figure 10 makes it possible to distinguish a double dynamics from front (saturated) and (unsaturated). The transport equation corresponds to a diagram of convection-diffusion which must make it possible to replace the diagram of pure convection [25]. Work is currently carried out to optimize this new algorithm of filling, in particular on the precise details concerning the hydrodynamic tensor of dispersion making it possible to integrate the effects of micro and macro voids.

6. Simulation of LCM processes and process/structure optimisation

To summarize the different works on the simulation of LCM processes, we present on Figure 11, a configuration of injection on a part including [a 3-D, multi-layers and non isothermal analysis].

Particular problems will concern to the analysis of draping with the influence of reinforcements shearing on the permeability, compressibility and thermal conductivity. Thermal simulation helps understand better the influence of the viscosity changes on the filling of the mold. It makes it possible to take into account the heat balance, the heat released by the chemical reaction of polymerization (Achim *et al.*, 2003). It gives important information on the resin choice, to ensure a good thermal regulation of the mould and to control the chemical reaction. One can thus modify the numerical parameters in order to find a sequence of correct mould filling with injection and vent optimized gates, to start the polymerization reaction at

the convenient period, as well as cooling. The cycle time can thus be reduced by an analysis of the health material optimization, making it possible to obtain parts of better quality with improved mechanical properties. The general framework of the Process/Structure coupling is defined of Figure 12. This figure lists some parameters controlling the process and the structure. Within the framework of optimization (Le Riche *et al.*, 2003), (Saouab *et al.*, 2002b), these parameters are variables and the physical properties are the optimization criteria. The variables describing the fibres position and the criteria of void content and polymerization are common.
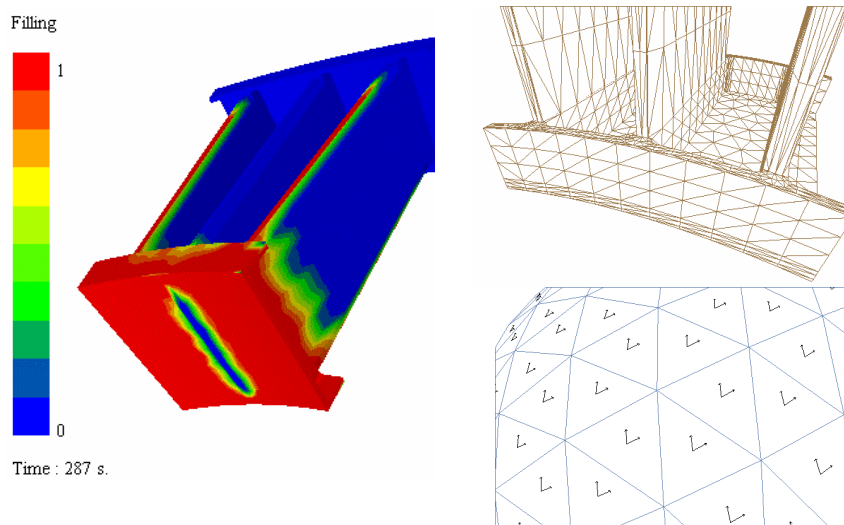

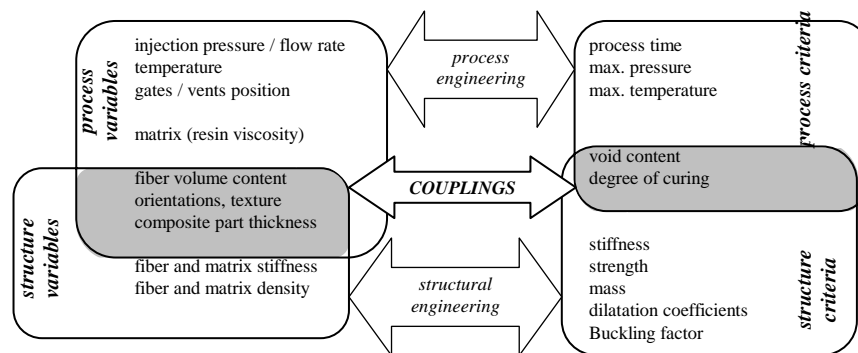**Figure 11.** *LCM injection analysis for multi layers part*

Figure 12. *Couplings examples between process and structure*

7. Conclusion

This work made it possible to draw a progress report about numerical modelling of LCM process. After describing the context and the framework of the various families of processes, we developed the main equations corresponding to THM couplings in porous media. Apart from the problems specific to thermal and the chemical kinetics, we analysed HM couplings, allowing to determine four great classes of problems concerning the continuity equation. The boundary and initial conditions were specified and also synthesized in a general table making it possible to compare RTM, LRI and RFI processes. We thus could develop some parametric analysis of the processes. In the field of the numerical methods, the pressure interpolation with discontinuous elements enables us to obtain perfectly conservative results. The conservative character of the results is crucial for LCM processes. The interpolation of traditional finite elements gives bad results with which nothing interesting can be concluded. With the new method, the mass conservation is ensured, even for the simplified meshes. The later developments would consist in employing interpolations of a higher nature to interpolate fields of displacement and to validate work concerning the coupling with residual stresses and total mechanical properties. Eventually, in the field of physical modelling, an effort of development must be made regarding the infusion processes, and more precisely RFI process in order to allow the integration of new infusion strategies, but also the integration of new behavior laws. The saturation analysis may also enable us to continue the development of a health material criterion. This would apply more precisely to the definition of optimal cycles. As for the thermal analysis, it is of primary importance to apprehend the minimization of cycle times, the improvement of the mechanical properties and the reduction of residual stresses in the composite part. In order to do this, studies should be initiated to couple simulation software of LCM processes with computer codes about structure and CAD analysis, thus informing a general reflexion on the choice of processes and materials.

8. Reference

Acheson J.A., Simacek P., Advani S.G., "The implication of fiber compaction and saturation on fully coupled VARTM simulation", *Composites Part A*, Vol. 35, 2003, pp. 159-169.

Achim V., Ruiz E., Soukane S., Trochu F., "Optimization of flow rate in Resin Transfert Molding", *Proceedings of the 8th Japan International SAMPE*, Tokyo, Japon, 2003.

Bailleul J-L., Sobotka V., Delaunay D., Jarny Y., "Inverse algorithm for optimal processing of composite materials", *Composites Part A*, Vol. 34, 2003, pp. 695-708.

Bear J., "Continuum Approach and Contaminant Transport in Ground Water Flows", *Modelling and Applications of Transport Phenomena in Porous Media,* Von Karman Institute for Fluid Dynamics, Lecture Series 1990-01, 1990.

Bickerton S., Abdullah M.Z., "Modeling and evaluation of the filling stage of the injection/compression molding", *Composites Science and Technology*, Vol. 63, 2003, pp. 1359-1375.

Binetruy C., Calcul et validation expérimentale de la perméabilité et prévision de l'imprégnation de tissus en moulage RTM, Thèse de Doctorat, Ecole des Mines de Douai, 1996.

Blest D.C, McKee S., Zulkifle A.K., Marshall P., "Curing simulation by autoclave resin infusion", *Composites Science and Technology*, Vol. 59, 1999, pp. 2297-2313.

Bréard J., Henzel Y., Trochu F., Gauvin R., "Analysis of dynamic flows through porous media. Part I: Comparison between saturated and unsaturated flows in fibrous reinforcements", *Polymer Composites*, Vol. 24, No. 3, 2003a, pp. 391-408.

Bréard J., Saouab A., Bouquet G., "Numerical simulation of void formation in LCM", *Composites Part A*, Vol. 34, 2003b, pp. 517-523.

Bréard J., Saouab A., Bouquet G., "Dependence of the reinforcement anisotropy on a three dimensional resin flow observed by X-Ray radioscopy", *Journal of Reinforced Plastics and Composites*, Vol. 18, No. 9, 1999, pp. 814-826.

Bréard J., Modélisation de la perméabilité/compressibilité des renforts fibreux et contrôle de la santé matière lors de la mise en forme des matériaux composites. Application à la simulation des procédés LCM "Liquid Composite Molding", Habilitation à diriger des Recherches, Université du Havre, 2004.

Bruschke M.V., Advani S.G., "A numerical approach to model non-isothermal viscous flow through fibrous media with free surfaces", *International Journal for Numerical Methods in Fluids*, Vol. 19, 1994, pp. 575-603.

Cadinot S., Aspects rhéologiques de la compressibilité d'un renfort fibreux pour matériaux composites : études en compression et relaxation, Thèse de doctorat, Université du Havre, 2002.

Chen B., Cheng AHD., Chou TW., "A non-linear compaction model for fibrous performs", *Composites Part A*, Vol. 32, No. 5, 2001, pp. 701-707.

Coussy O., *Mécanique des Milieux Poreux*, Éditions Technip, 1991.

Farina A., Preziosi L., "Non-isothermal injection molding with resin cure and preform deformability", *Composites Part A*, Vol. 31, 2000, pp. 1355-1372.

Fournier R., Optimisation du procédé RTM, Thèse de doctorat, CEMEF-Ecole des Mines de Paris, 2003.

Gao D.M., Trochu F., Gauvin R., "Numerical analysis of the Resin Transfer Molding process by the finite element method", *Advances in Polymer Technology*, Vol. 12, No. 4, 1993, pp. 329-342.

Hill R., Muzumar S., Lee L., "Analysis of volumetric changes of unsaturated polyester resin during curing", *Polymer Eng. And Sci.*, Vol. 35, No. 10, 1995, pp. 852-859.

Kang M.K., Lee W.L., "A flow front refinement technique for the numerical simulation of the Resin Transfert Molding process", *Composites Science and Technology*, Vol. 59, 1999, pp. 1663-1674.

Kang M.K., Lee W.L., "Analysis of vacuum bag Resin Transfer Molding process", *Composites Part A*, Vol. 32, 2001, pp. 1553-1560.

Labat L., Bréard J., Pillut-Lesavre S., Bouquet G., "Void fraction prevision en LCM parts", *European Physical Journal- Applied Physics* , Vol. 16, No. 2, 2001, pp. 269-279.

Lacoste E., Mantaux O., Danis M., "Numerical simulation of metal matrix composites and polymer matrix composites processing by infiltration : a review", *Composites Part A*, Vol. 33, 2002, pp. 1605-1614.

Le Riche R., Saouab A., Bréard J., "Coupled RTCM and composite layup optimization", *Composites Science and Technology*, Vol. 63, 2003, pp. 2277-2287.

Lomov S.V., Huysmans G., Luo Y., Parnas R.S., Prodromou A., Verpoest I., Phelan F.R., "Textiles composites : modelling strategies", *Composites Part A*, Vol. 32, 2001, pp. 1379-1394.

Loos A.C., MacRae J.D., "A process simulation model for the manufacturing of a blade-stiffened panel by the resin film infusion process", *Composites Science and Technology*, Vol. 56, 1996, pp. 273-288.

Maier R., Rohaly T., Advani S., Fickie K., "A fast numerical method for isothermal Resin Transfer Molding filling", *Int. Journal for Numerical Methods in Eng.*, Vol. 39, 1996, pp. 1405-1417.

Ngo N.D., Tamma K.K., "Non isothermal 2D flow/3D thermal developments encompassing process modelling of composites: flow/thermal/cure formulations and validations", *International Journal for Numerical Methods in Engineering*, Vol. 50, 2001, pp. 1559-1585.

Park J., Kang M.K., "A numerical simulation of the resin film infusion", *Composite Structures*, Vol. 60, 2003, pp. 431-437.

Patel N., Lee LJ., "Modeling of void formation and removal in liquid composite molding. Part II: model development and implementation", *Polymer Composites*, Vol. 17, No. 1, 1996, pp. 96-103.

Pham X.T, F. Trochu, "Simulation of compression resin transfer molding to manufacture thin composite shells", *Polymer Composites*, Vol. 20, No. 3, 1999, pp. 436-459.

Pitchumani R., Ramakrishanan B., "A fractal geometry model for evaluating permeabilities of porous preforms used in LCM", *Int. J. of Heat and Mass Transfer*, Vol. 42, 1999, pp. 2219-2232.

Ryan M.E., Dutta A., "Kinetics of epoxy cure: a rapid technique for kinetic parameter estimation", *Polymer*, Vol. 20, 1979, pp. 203-206.

Remacle J-F., Bréard J., Trochu F., "Numerical analysis of the Liquid Composite Molding by LCMFLOT", *Proceedings of the 5th Conference on Flow Process in Composite Materials*, Plymouth, Angleterre, 1999.

Remacle J-F., Bréard J., Trochu F., "A natural way to simulate flow driven injections in Liquid Composite Molding", *Proceedings of the 6th International Conference on Computer Methods in Composite Materials*, Montréal, Canada, 1998, In Computer Methods in Composite Materials VI, pp. 97-107.

Ruiz E., De la caractérisation des matériaux et simulation du procédé à l'optimisation de la fabrication des composites par injection sur renfort, PhD, Ecole Polytechnique de Montréal, 2004.

Saouab A., Bréard J., Bouquet G., "Contribution to the optimization of RTM and CRTM processes", *Proceedings of the 5th International ESAFORM*, Krakow, Pologne, 2002a.

Saouab A., Le Riche R., Bréard J., "Couplage procédé propriétés: analyse d'une plaque composite", *Revue des Composites et Matériaux Avancés*, Vol. 12, No. 3, 2002b, pp. 515-529.

Sevostianov I.B., VerijenkoV.E., von Klemperer C.J., "Mathematical model of cavitation during resin film infusion process", *Composite Structures*, Vol. 48, 2000, pp. 197-203.

Spaid M., Phelan F., "Modeling void formation dynamics in fibrous porous media with the Lattice Boltzmann method", *Composites Part A*, Vol. 29, No. 7, 1998, pp. 749-755.

Torres Carot R., Boust F., Poitou A., "The concept of permeability in the Resin Transfert Molding process: Darcy's law and multiple porosity", *Publications de l'ONERA*, 2001.

Tucker C., "Heat Transfer and reaction issues in Liquid Composite Molding", *Polymer Composites*, Vol. 7, No. 1, 1996, pp. 60-72.